Supporting Information

Two for the Price of One: Heterobivalent Ligand Design Targeting Two Binding Sites on Voltage-Gated Sodium Channels Slows Ligand Dissociation and Enhances Potency

Alicia Peschel, [†, #] Fernanda C. Cardoso, [†, #] Andrew A. Walker, [†] Thomas Durek, [†] M. Rhia L. Stone, [†] Nayara Braga Emidio, [†] Philip E. Dawson, [§] Markus Muttenthaler, [*, †, ‡] and Glenn F. King [*, †]

[†] Institute for Molecular Bioscience, The University of Queensland, St Lucia, QLD 4072, Australia

[§] Department of Chemistry, The Scripps Research Institute, La Jolla, CA, USA

[‡] Institute of Biological Chemistry, Faculty of Chemistry, University of Vienna, 1090 Vienna, Austria

[#] equal contributions

*** corresponding authors:**

A/Prof. Markus Muttenthaler, Institute of Biological Chemistry, Faculty of Chemistry, University of Vienna, 1090 Vienna, Austria. Phone (+43) 1 4277 70515; Email: markus.muttenthaler@univie.ac.at.

Prof. Glenn King, Institute for Molecular Bioscience, The University of Queensland, St Lucia, QLD 4072, Australia. Phone (+61) 7 3346-2025; Email: glenn.king@imb.uq.edu.au.

Table of Contents

Supporting Figures

Supporting Table

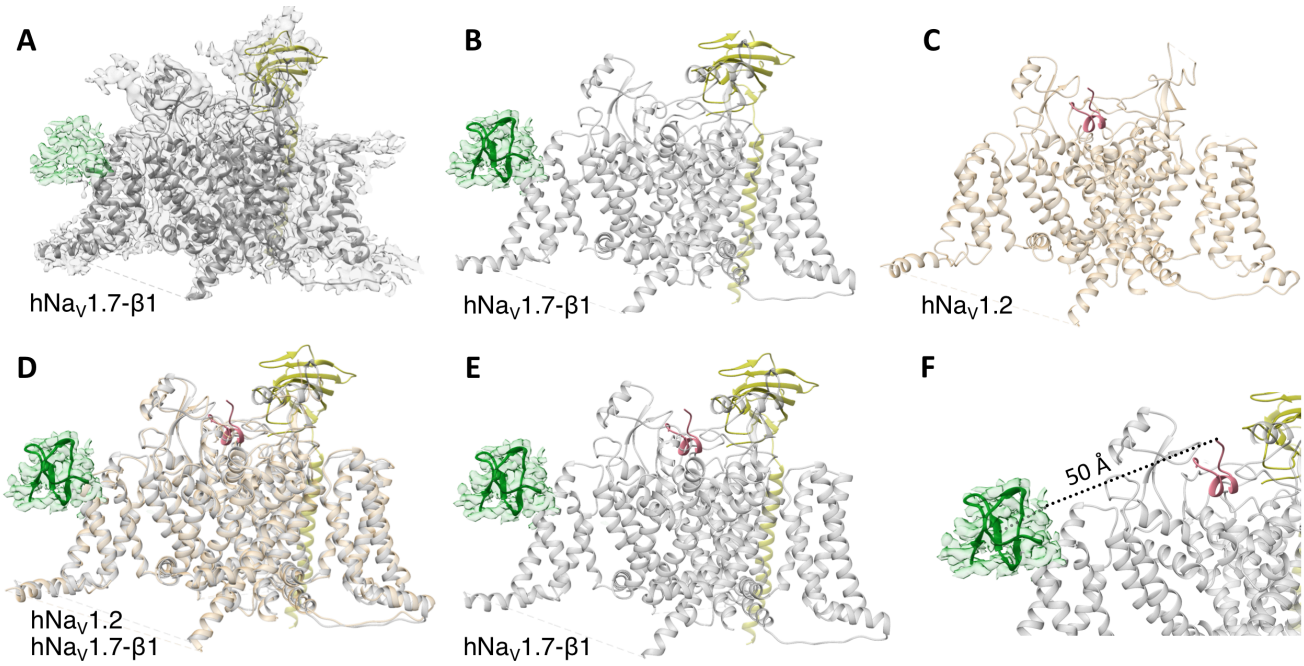

Figure S1: Cryo-electron microscopy structures for determination of suitable linker length. (A) $hNa_V1.7$-β1 complex and overall electron density map in surface style. (B) $hNa_V1.7$-β1 with electron density blob for HwTx-IV (green) above VSD_{II}.[1] The m_3-HwTx-IV peptide has been randomly positioned in this blob of density as accurate docking of the toxin structure was not possible due to the unknown binding sites and interactions. (C) $hNa_V1.2$ bound to μ-KIIIA (magenta).[2] (D) $hNa_V1.7$-β1 and $hNa_V1.2$ were aligned in Chimera to obtain μ-KIIIA's position in $hNa_V1.7$-β1 (alignment algorithm: Needleman-Wunsch; matrix: BLOSUM-62). (E) $hNa_V1.7$-β1 in the presence of m_3-HwTx-IV and μ-KIIIA. (F) Zoomed in view with measured distance of ~50 Å between the center of the HwTx-IV density blob and the N-terminus of μ-KIIIA (PDB IDs 5T3M, 6J8E, 6J8G and EMD-9781).

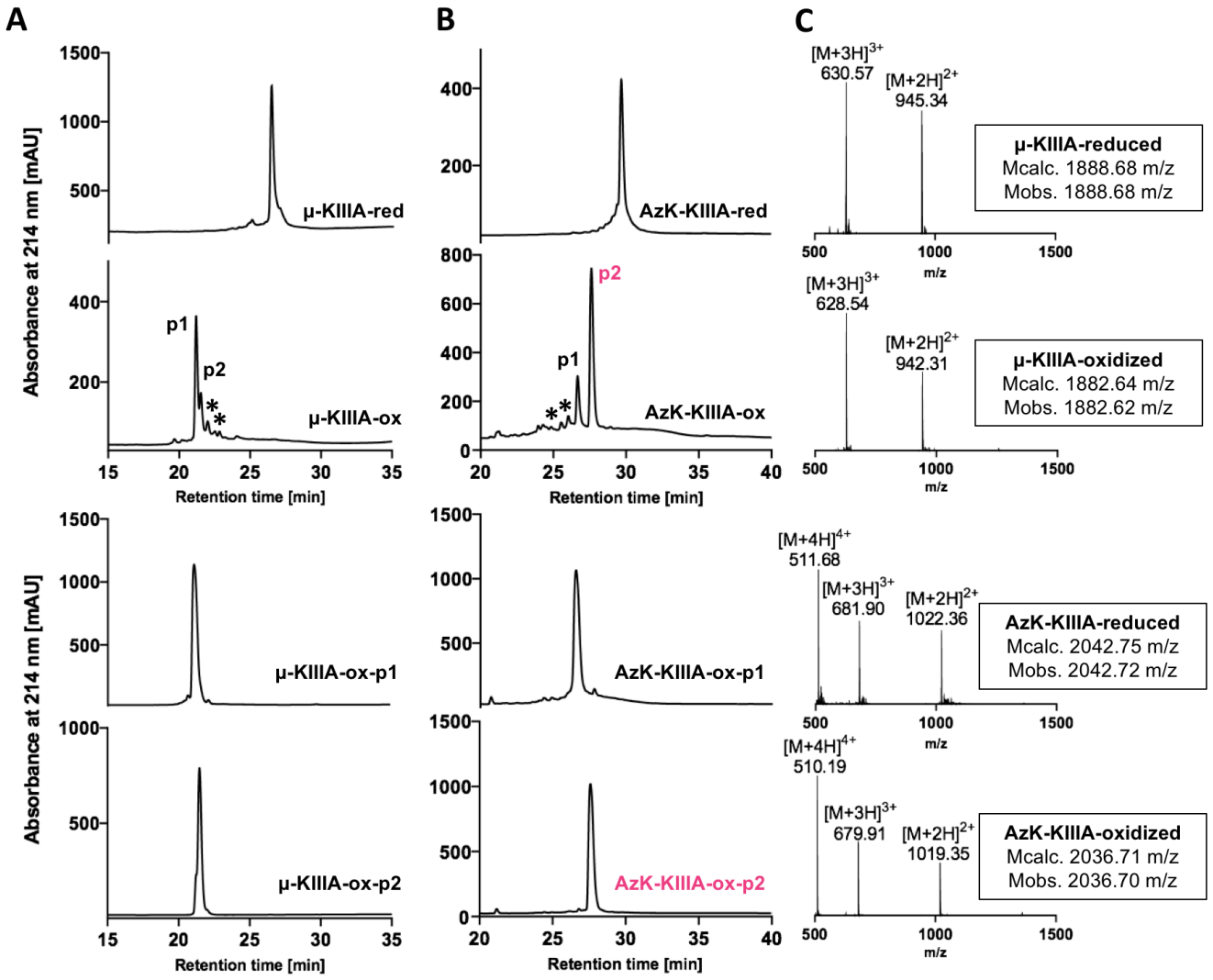

Figure S2: Characterization of reduced and folded μ-KIIIA and AzK-KIIIA peptides. (A, B) RP-HPLC chromatograms of the reduced and folded peptides. After oxidative folding of the reduced peptides, two distinct peaks (p1 and p2) with identical monoisotopic mass values (1882.62 Da for μ-KIIIA, 2036.70 Da for AzK-KIIIA) were obtained on analytical RP-HPLC. This oxidative folding pattern of μ-KIIIA has been previously reported,[3] with the major product (p1) adopting a (Cys^{I}–Cys^{V}, Cys^{II}–Cys^{IV}, Cys^{III}–Cys^{VI}) connectivity and the minor product (p2) adopting a (Cys^{I}–Cys^{VI}, Cys^{II}–Cys^{IV}, Cys^{III}–Cys^{V}) connectivity. Other minor oxidative side products (*) were not characterized. AzK-KIIIA peptide used for bioorthogonal ligation is colored in magenta. RP-HPLC was performed using an analytical C_{18} column at a flow rate of 0.2 mL/min and a 1% linear gradient ranging from 0 to 35% or 40% solvent B, where solvent A was 0.05% TFA in water, and solvent B was 0.043% TFA in 90/10% (v/v) acetonitrile/water. UV absorbance was monitored at 214 nm. (C) LC-ESI-MS (positive ion mode) spectra of the linear and oxidized peptides obtained on a high-resolution mass spectrometer. p: RP-HPLC peak; red: reduced peptide; ox: oxidized peptide; Mcalc.: calculated ion mass; Mobs.: experimentally observed ion mass.

Table S1: Inhibitory potency of μ-KIIIA and AzK-KIIIA analogues at $hNa_V1.7$ determined by electrophysiology using a QPatch 16X automated patch-clamp system. The major folding product of AzK-KIIIA (μ-KIIIA-ox-p2) used for bioorthogonal conjugation is highlighted in bold. The IC_{50} values are mean (in nM) ± SEM of *n* number of independent experiments. p: RP-HPLC peak.

Ligands	IC_{50} [nM] (mean ± SEM)	*n*
$hNa_V1.7$		
μ-KIIIA-ox-p1	132 ± 37	4
μ-KIIIA-ox-p2	154 ± 15	3
AzK-KIIIA-ox-p1	934 ± 572	3
AzK-KIIIA-ox-p2	**96 ± 41**	**3**

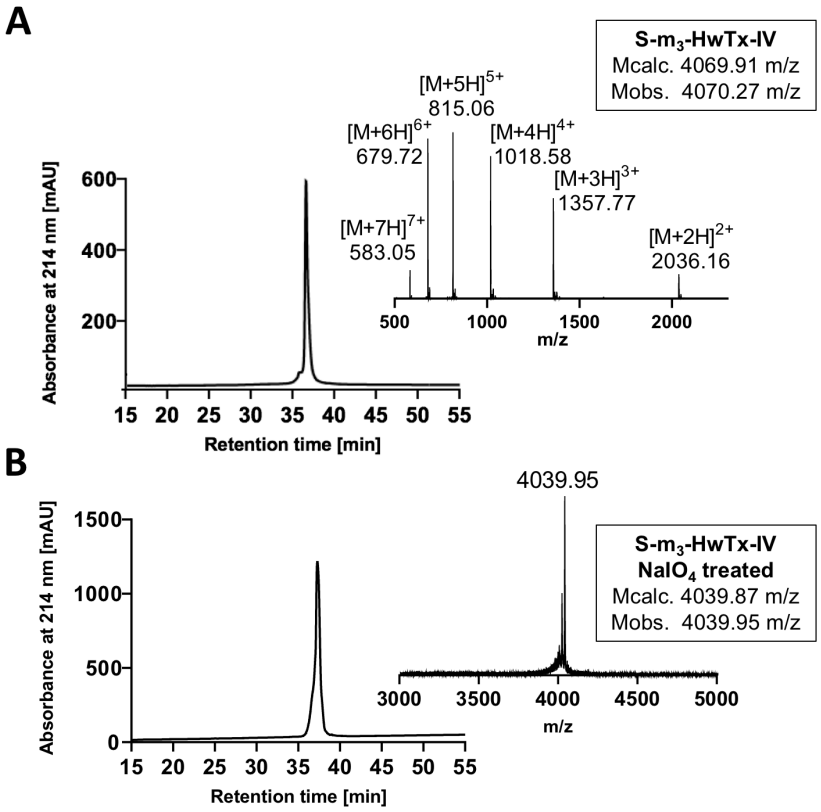

Figure S3: Analytical HPLC chromatograms and MS analysis of S-m_3-Huwentoxin-IV. (A) and sodium periodate treated S-m_3-Huwentoxin-IV (B). RP-HPLC was performed using an analytical C_{18} column at a flow rate of 0.2 mL/min over a 1% linear gradient ranging from 0 to 55% solvent B. Solvent A was 0.05% TFA in water, and solvent B was 0.043% TFA in 90/10% (v/v) acetonitrile/water. LC-ESI-MS (positive ion mode) was performed on a high-resolution mass spectrometer for S-m_3-Huwentoxin-IV and MALDI-TOF analysis was performed for sodium periodate treated S-m_3-Huwentoxin-IV. Mcalc: calculated ion mass; Mobs: experimental observed ion mass.

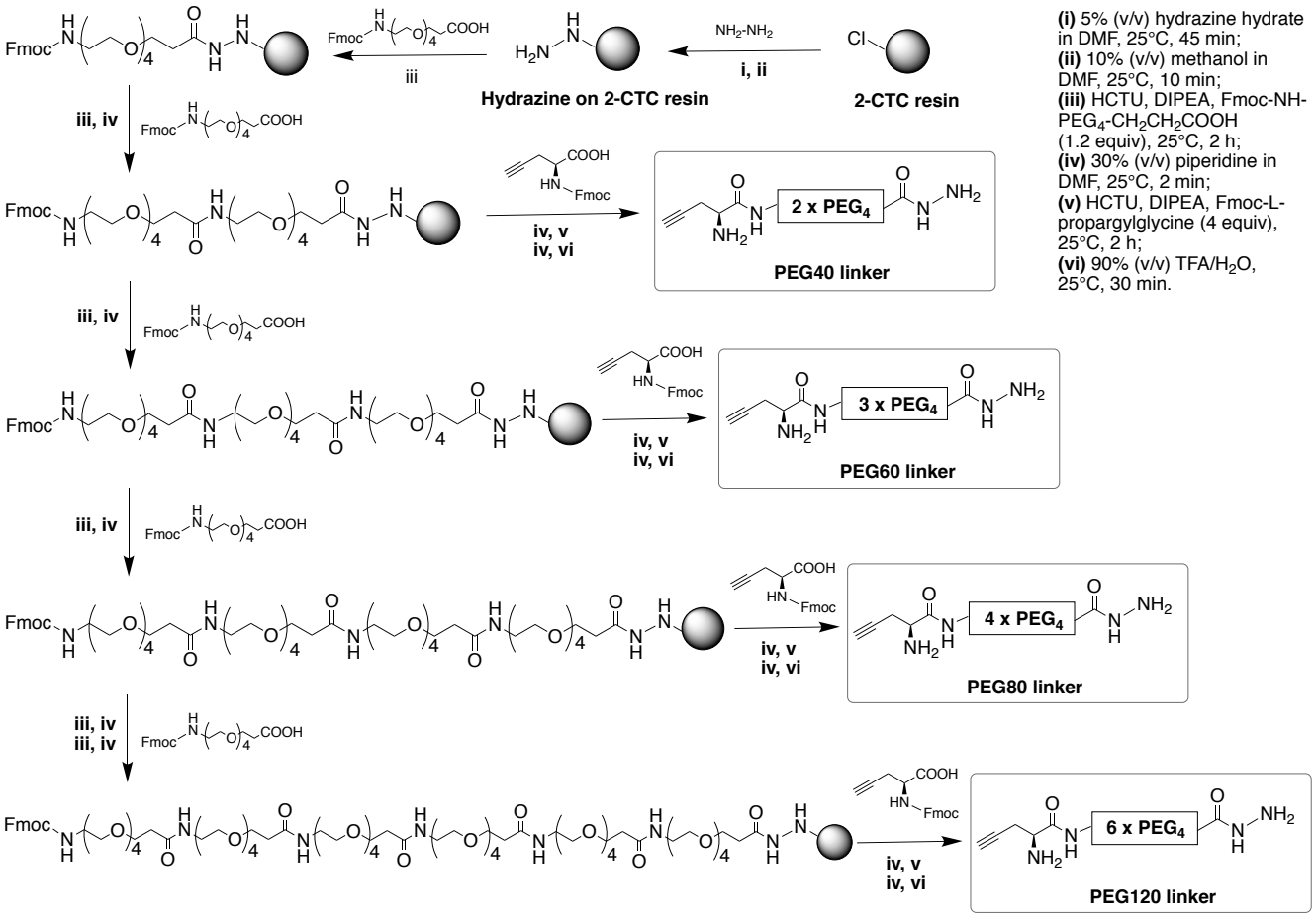

Figure S4: Details of linker synthesis scheme to produce heterobifunctionalized (alkyne and hydrazide) polyethylene glycol (PEG) linkers. 2-Chlorotrityl chloride (2-CTC) resin was converted to 2-chlorotrityl hydrazine resin. Unreacted sites were capped with an excess of methanol. Couplings of Fmoc-protected PEG_4 were carried out using standard Fmoc-SPPS protocols. Fmoc-L-propargylglycine was used as the final amino acid to incorporate an alkyne moiety. The PEG linkers were cleaved with TFA and purified using RP-HPLC.

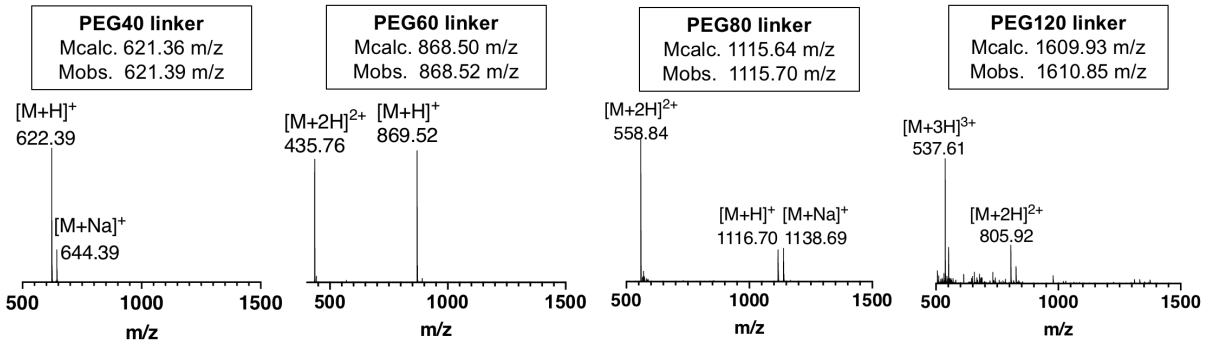

Figure S5: Characterization of PEG linkers. ESI-MS spectra of PEG linkers observed with LC-ESI-MS (positive ion mode) on a high-resolution API Qstar Pulsar mass spectrometer (PerkinElmer Sciex, Foster City, USA). In the PEG40 and PEG80 spectra, sodium adducts (+22) were observed for PEG40 (622.4) and PEG80 (1116.6). Mcalc: calculated ion mass; Mobs: experimental observed ion mass.

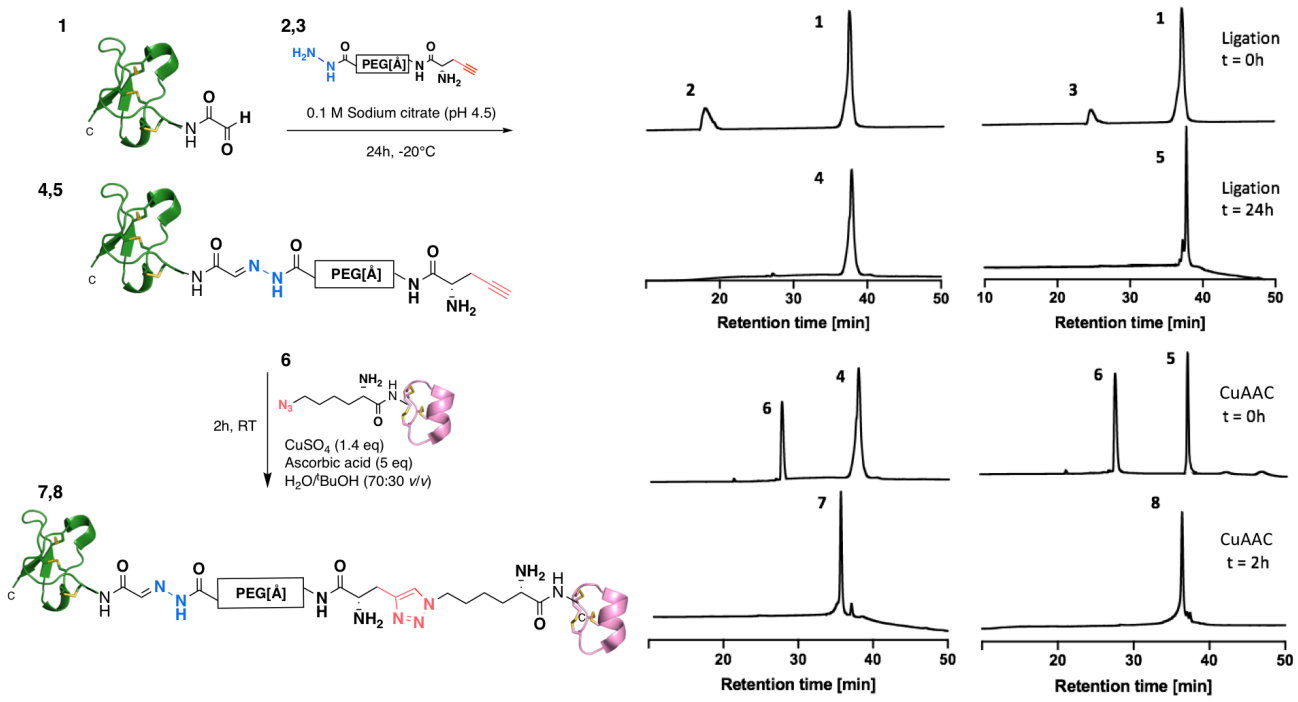

Figure S6: Conjugation of m_3-HwTx-IV to KIIIA via a heterobifunctional PEG linker using bioorthogonal hydrazide ligation and copper-assisted azide-alkyne cycloaddition. PEG40 linker **2** and PEG80 linker **3** were ligated with aldehyde-m_3-HwTx-IV **1**. The reaction was allowed to proceed for 24 h, which resulted in a 95% conversion for **2**+**1** and a 70% conversion for **3**+**1** (79% conversion for [m_3-HwTx-IV]-[PEG60]-[K-KIIIA]+**1** and 68% conversion for [m_3-HwTx-IV]-[PEG120]-[K-KIIIA]+**1**, data not shown). The ligated products [m_3-HwTx-IV]- [PEG40] **4** and [m_3-HwTx-IV]- [PEG80] **5** were purified, followed by the CuAAC chemistry with AzK-KIIIA **6**. After 2 h, a triazole linkage was formed to yield the desired products [m_3-HwTx-IV]-[PEG40]-[K-KIIIA] **7** and [m_3-HwTx-IV]-[PEG80]-[K-KIIIA] **8**. RP-HPLC was performed using an analytical C_{18} column at a flow rate of 0.2 mL/min and a 1% linear gradient ranging from 0 to 50% solvent B, where solvent A was 0.05% TFA in water, and solvent B was 0.043% TFA in 90/10% (v/v) acetonitrile/water. UV absorbance was monitored at 214 nm.

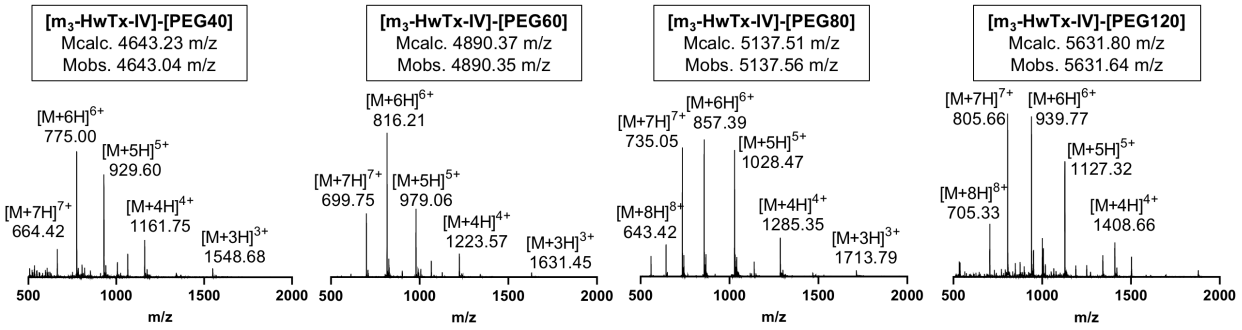

Figure S7: Characterization of the hydrazone ligation reaction. ESI-MS spectra of [m_3-HwTx-IV]-[PEG[Å]] observed with LC-ESI-MS (positive ion mode) on a high-resolution API Qstar Pulsar mass spectrometer (PerkinElmer Sciex, Foster City, USA). Mcalc: calculated ion mass; Mobs: experimental observed ion mass.

A

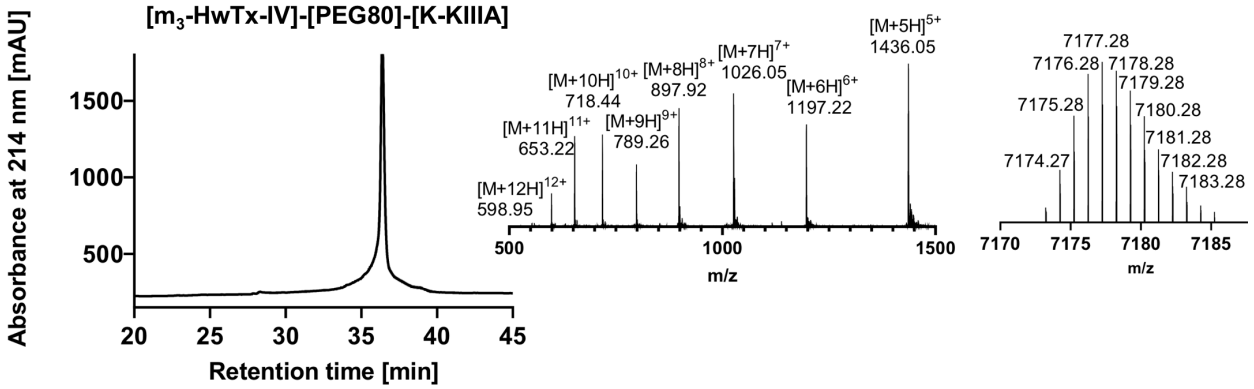

B

Ligand	Linker Length	Mcalc. [m/z]	Mobs. [m/z]
[m_3-HwTx-IV]-[PEG40]-[K-KIIIA]	45 Å	6679.95	6679.96
[m_3-HwTx-IV]-[PEG60]-[K-KIIIA]	64 Å	6927.09	6927.11
[m_3-HwTx-IV]-[PEG80]-[K-KIIIA]	**84** Å	7174.23	7174.27
[m_3-HwTx-IV]-[PEG120]-[K-KIIIA]	123 Å	7668.52	7668.42
[m_3-HwTx-IV]-[PEG80]	84 Å	5137.51	5137.56
[K-KIIIA]-PEG80]	84 Å	3153.31	3153.32

Figure S8: Analytical RP-HPLC chromatogram and high-resolution mass spectra of [m_3-HwTx-IV]-[PEG80]-[K-KIIIA], and table of calculated and observed masses of all conjugated ligands. (A) RP-HPLC chromatogram and ESI-MS spectrum observed with LC-ESI-MS (positive ion mode) and reconstructed mass spectrum for [m_3-HwTx-IV]-[PEG80]-[K-KIIIA] using a high-resolution TripleTOF 5600 mass spectrometer (AB Sciex). (B) Linker lengths (measured with Avogadro software[4]) and calculated and observed mass values for the bivalent ligands and controls. RP-HPLC was performed using analytical C_{18} column at a flow rate of 0.2 mL/min and a 1% linear gradient ranging from 0 to 45% solvent B, where solvent A was 0.05% TFA in water, and solvent B was 0.043% TFA in 90/10% (v/v) acetonitrile/water. Mcalc.: calculated ion mass; Mobs.: experimental observed ion mass.

References

(1) Shen, H.; Liu, D.; Wu, K.; Lei, J.; Yan, N. Structures of human $Na_V1.7$ channel in complex with auxiliary subunits and animal toxins. *Science* **2019,** 363, 1303–1308.

(2) Pan, X.; Li, Z.; Huang, X.; Huang, G.; Gao, S.; Shen, H.; Liu, L.; Lei, J.; Yan, N. Molecular basis for pore blockade of human Na^+ channel $Na_V1.2$ by the μ-conotoxin KIIIA. *Science* **2019,** 363, 1309–1313.

(3) Khoo, K. K.; Gupta, K.; Green, B. R.; Zhang, M. M.; Watkins, M.; Olivera, B. M.; Balaram, P.; Yoshikami, D.; Bulaj, G.; Norton, R. S. Distinct disulfide isomers of μ-conotoxins KIIIA and KIIIB block voltage-gated sodium channels. *Biochemistry* **2012,** 51, 9826–9835.

(4) Hanwell, M. D.; Curtis, D. E.; Lonie, D. C.; Vandermeersch, T.; Zurek, E.; Hutchison, G. R. Avogadro: an advanced semantic chemical editor, visualization, and analysis platform. *J. Cheminform.* **2012,** 4, 17.